

A Coordinated Design of PSSs and UPFC-based Stabilizer Using Genetic Algorithm

Lokman H. Hassan
Member, IEEE
University of Duhok
Duhok, Kurdistan Region,
Iraq
lokmanhadi@ieee.org

M. Moghavvemi
University of Malaya
50603 Kuala Lumpur,
Malaysia
mahmoud@um.edu.my

Haider A.F. Almurib
Senior Member, IEEE
The University of
Nottingham
43500 Semenyih, Malaysia
haider.almurib@ieee.org

K. M. Muttaqi
Senior Member, IEEE
University of Wollongong,
New South Wales,
NSW 2522, Australia
kashem@uow.edu.au

Abstract -- This paper details a new coordinated design between Power System Stabilizers (PSSs) and Unified Power Flow Controller (UPFC) using Genetic Algorithms (GA). The GA scheme determines the optimal location for the UPFC while tuning its control parameters, resulting in the optimization of the quantity, parameters and locations of the PSSs under different operating conditions. The problem is formulated as a multi-objective optimization problem in order to maximize the damping ratio(s) of the electromechanical modes, matching different numbers of PSSs with UPFC. The approach is successfully tested on the New England-New York interconnected system (16-machine and 68-bus), proving its effectiveness in damping local and inter-area modes of oscillations.

Index Terms-- Genetic algorithms, Low-frequency oscillations, Optimization, Power system stability, Power system control, Power transmission, PSS, UPFC.

I. INTRODUCTION

A modern power system is a large, nonlinear and complex system and it is subject to different kinds of events which result in low-frequency oscillations in a power system that will affect the system stability. Engineers and researchers are continually tasked to find a simple, effective and economical strategy to stabilize power system(s) [1]. This resulted in the emergence of a Power System Stabilizer (PSS), where a supplementary stabilizing signal is added to excitation system, making it simple and economically favorable [2-4].

As a result of the rapid growth of the development of solid-state power electronics and advanced digital controllers, the current deregulated electrical market offers Flexible Alternating Current Transmission Systems (FACTS) devices [5]. These devices, working at high speeds, can decisively control a power system [6, 7], and improve transient stability, steady-state stability, voltage stability, and dampen low-frequency oscillations.

Although the main function of the FACTS controller is not damping of the low-frequency oscillations, adding an auxiliary controller to FACTS will considerably increase the power system damping [8, 9]. PSS and FACTS devices are the most used tools to improve the small-signal stability, and consequently, the stability of power systems. However, the damping of power system oscillations is affected by setting

the parameters of PSSs and/or FACTS-based stabilizers and the selection of the number of these stabilizers and their location within the network [10, 11]. In addition, a coordinated design among stabilizers should be considered when a combination of devices is involved [12, 13]. Among all the FACTS devices, unified power flow controller (UPFC) is capable of simultaneously controlling the bus voltage, the phase angle, and the transmission line impedance, making it applicable in power-flow control and power system stabilizing control [14]. Considering the limitations of the conventional and optimal controllers and due to the fact that the voltage control of the DC link capacitor inside the UPFC interacts negatively with the PSS [12], a design that coordinates the PSS and UPFC damping controller with intelligent optimization based multi-objective functions to select their optimal location, number and parameters is required.

The coordinated design of the PSS(s) and FACTS-based stabilizers are significantly more efficient in damping oscillations and improving stability compared to an individual design of these stabilizers [12, 13]. Artificial Intelligence (AI) techniques emerged in power systems as effective tools to solve many complex problems, but AIs can be even more effective when coupled with conventional mathematical approaches [15]. In order to study the coordinated effect of a UPFC and PSS in the system, an adaptive control scheme was used by Mishra [16] for the UPFC by applying a new H_∞ to a single-neuron radial basis function neural network. A Genetic Algorithm (GA) was used to optimize the coefficient of the auxiliary signal, its error, and the difference of error. The proposed controller was applied to a four-machine power system equipped with only one PSS.

Power system managers and researchers still prefer the lead-lag control structure due to the ease of its online tuning parameters such as structure and reliability when implemented in real power systems. Low-frequency oscillations can be sufficiently damped by the appropriate selection of conventional lead-lag controller parameters [17]. GAs have been successfully applied to tune such conventional controller parameters [11, 13, 18]. A robust

coordinated design of a PSS and static VAR compensator-based stabilizer [18], and a robust coordinated design of a PSS and Thyristor Controlled Series Capacitor (TCSC)-based stabilizer [13] were applied to a power system. In both approaches, a real-coded GA was employed to search for the optimal parameters of the stabilizers. In order to estimate the effectiveness of the proposed approaches, the singular value decomposition technique was used to measure the controllability of the electromechanical modes. However, both approaches were tested only on a single machine infinite bus system.

In this paper, a new coordination algorithm, using GA for coordination among the PSSs, and between PSSs and UPFC-based stabilizer is proposed. A multi-objective function has been proposed to formulate the problem in order to maximize the damping ratio of the electromechanical modes over a wide range of operating conditions. In order to guarantee the robustness of the proposed approach, several scenario-conditions have been used in the optimization process. The proposed coordinated design between PSSs and the UPFC, will aim to increase the minimum damping ratio, compared to the system installed with only PSSs, and will target reducing the number of PSSs required for the system. The approach is successfully tested on the New England-New York interconnected system (16-machine and 68-bus) to verify its effectiveness in damping local and inter-area modes of oscillations.

II. PROBLEM FORMULATION

The linearized Heffron-Phillips model [12, 19] is used for several operating-conditions to represent the power system with installed PSSs and a UPFC-based stabilizer. For every operating condition, a linearized model can be written in the state space form as given below

$$\dot{x} = Ax + Bu \quad (1)$$

$$y = Cx + Du \quad (2)$$

where the state matrix is designated by (A), the input matrix by (B), the control vector by (u), the state vector by (x), the output matrix by (C), the feed-forward matrix by (D) and the output signals vector by (y).

For a closed-loop system where $e_r(s)$ is the error signal, and $r_f(s)$ is the reference input, the controller K_a can be expressed in the state-space form as

$$\dot{x}_p = A_p x_p + B_p e_r \quad (3)$$

$$u = C_p x_p + D_p e_r \quad (4)$$

where x_p is the state vector of the controller.

Combining (3) and (4) with (1) and (2), the closed-loop system is obtained

$$\dot{x}_c = A_c x_c \quad (5)$$

where $x_c = [x \ x_p]^T$ is the state vector of the closed-loop system.

The damping ratio (ζ_i) of the closed-loop i -th eigenvalue (λ_i) can be therefore described as

$$\zeta_i = \frac{-\sigma_i}{\sqrt{\sigma_i^2 + \omega_{ni}^2}} \quad (6)$$

where σ_i and ω_{ni} are real and imaginary parts of the λ_i .

A. Inclusion of PSSs

Fig. 1 shows a block diagram of a typical PSS. The transfer function of the i -th two stages lead-lag PSS is [11]

$$\Delta u_{PSS,i} = \frac{sK_{PSSi}T_{wi}}{1+sT_{wi}} \frac{(1+\left(\frac{\sqrt{\gamma_i}}{\eta_i}\right)s)^2}{(1+\left(\frac{1}{\eta_i\sqrt{\gamma_i}}\right)s)^2} \Delta \omega_i \quad (7)$$

where Δu_{PSS} is the output signal of the PSSs, K_{PSSi} is the gain of i -th PSS stabilizer, T_w is the time constant of the washout circuit, and time constants T_{1i} and T_{2i} are $\sqrt{\gamma_i}/\eta_i$ and $1/\eta_i\sqrt{\gamma_i}$ respectively.

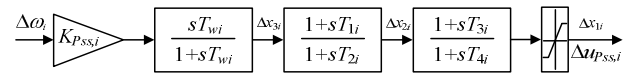


Fig.1. Power system stabilizer.

By adding the state variables of the PSSs ($[\Delta x_1 \ \Delta x_2 \ \Delta x_3]$) to the system's state variables without stabilizers ($\dot{x} = Ax$), the closed-loop system matrix is formed, where the variables with the prefix Δ are n-order vectors.

B. Inclusion of UPFC

In this paper, the flux-decay model is used to model the UPFC-based stabilizer into the power systems. For this, proper and complete structures are considered for designing the UPFC damping controller. The UPFC comprises two Voltage Source Converters (VSCs), two transformers (i.e. excitation and boosting), and a DC storage capacitor. The input control signals for both converters are the excitation amplitude modulation ratio and the excitation phase angle for the first converter, and the boosting amplitude modulation ratio and the boosting phase angle for the second converter. An efficient way of controlling the UPFC is through the excitation phase angle (δ_E), [20, 21]. A conventional PI and a lead-lag controller are adapted to implement the damping controller. In addition, it is imperative to balance the power between the two converters, which is done through controlling the voltage across the DC link capacitor. This is done using a PI controller to modulate the excitation angle δ_E . The overall controller system is shown in Fig. 2.

In Fig. 2, the time constants T_a and T_b can be assigned the values $\sqrt{\alpha}/\beta$ and $1/\beta\sqrt{\alpha}$ respectively. Here, we use a two stage compensator and make them identical for simplicity,

i.e. $T_c = T_a$ and $T_d = T_b$. This is mainly because in many practical cases the phase lead or lag required is greater than that obtainable from a single lead or lag network and in general two or three cascaded lead stages are used, [22]. Please note that gain K_s has the value of 1 and that parameter T_s is the time delay representing the characteristics of the main circuit and control system [8].

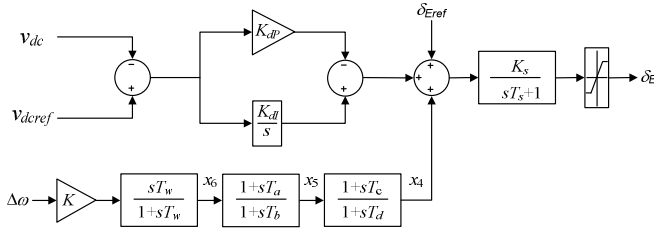


Fig. 2. Lead-lag controller with DC voltage regulator.

The closed-loop system matrix is obtained by adding the state vector of the UPFC damping controller ($[\Delta v_{dc} \Delta x_4 \Delta x_5 \Delta x_6 \Delta \delta_E]$) to the system's state variables without stabilizers.

C. Inclusion of UPFC and PSSs

Controlling the DC voltage inside the UPFC is necessary, but such control may interact negatively with the PSSs. Therefore, a design that coordinates PSSs and the UPFC damping controller must be taken into consideration [12]. The proposed optimization method provides a sound solution to the problem.

The closed-loop system matrix is obtained by adding the state vector of the PSSs and the state vector of the UPFC damping controller, to the system's state variables without stabilizers. Therefore, the closed-loop state matrix of an n-machine power system installed with PSSs and a UPFC can be obtained as given by (8), where D , T'_{do} , K_A , T_A , and identity matrix (I) are diagonal matrices; i is the machine number from which the controller's input signal is taken; and

$$x_c = [\Delta \delta \Delta \omega \Delta E'_q \Delta E'_{fd} \Delta x_1 \Delta x_2 \Delta x_3 \Delta v_{dc} \Delta x_4 \Delta x_5 \Delta x_6 \Delta \delta_E]^T, [8].$$

In (8), $K_1 - K_9$, K_{Pd} , K_{qd} , K_{vd} , $K_{p\delta e}$, $K_{q\delta e}$, $K_{v\delta e}$, and $K_{c\delta e}$ are linearization constants defined as:

$$\begin{aligned} K_1 &= \frac{\partial P_e}{\partial \delta}; & K_2 &= \frac{\partial P_e}{\partial E'_q}; & K_3 &= \frac{\partial E'_q}{\partial E'_q}; & K_{Pd} &= \frac{\partial P_p}{\partial v_{dc}} \\ K_4 &= \frac{\partial E'_q}{\partial \delta}; & K_5 &= \frac{\partial v_t}{\partial \delta}; & K_6 &= \frac{\partial v_t}{\partial E'_q}; & K_{qd} &= \frac{\partial E'_q}{\partial v_{dc}} \\ K_7 &= \frac{\partial \dot{v}_{dc}}{\partial \delta}; & K_8 &= \frac{\partial \dot{v}_{dc}}{\partial E'_q}; & K_9 &= \frac{\partial \dot{v}_{dc}}{\partial v_{dc}}; & K_{vd} &= \frac{\partial V_t}{\partial v_{dc}} \\ K_{p\delta e} &= \frac{\partial P_p}{\partial \delta_e}; & K_{q\delta e} &= \frac{\partial P_p}{\partial \delta_e}; & K_{v\delta e} &= \frac{\partial V_t}{\partial \delta_e}; & K_{c\delta e} &= \frac{\partial \dot{v}_{dc}}{\partial \delta_e} \end{aligned}$$

The purpose of the GA method is to obtain optimal coordination between the PSSs and the UPFC-based stabilizer. Determining the optimal values for K_{PSS} , γ , η , K , α , β , K_{dP} and the PSSs locations is the main purpose of the optimization.

III. THE PROPOSED OPTIMIZATION ALGORITHM

Evolutionary Genetic algorithms are global heuristics search methods that are employed to search for optimal or near optimal solutions for a multitude of problems. Like any other optimization scheme, GAs require an objective function. In this work, a GA method is used to propose a new method of coordinating UPFC and PSSs. The objective function of the proposed GA aims at achieving satisfactory damping over a wide operating conditions range for all operating modes. The proposed scheme using GA, is illustrated in Fig. 3. The minimum value of the damping ratio that provides satisfactory safety margin is chosen to be 0.05, [23].

As can be seen from the flowchart of Fig. 3, after initialization, the algorithm first generates the population which consists of chromosomes that represent the PSSs and UPFC-based stabilizer parameters and the location index (ℓ_o). In other words, a chromosome is a collection of

$$A_c = \begin{bmatrix} 0 & \omega_R I & 0 & 0 & 0 & 0 & 0 & 0 & 0 & 0 & 0 & 0 & 0 \\ -M^{-1}K_1 & -M^{-1}D & -M^{-1}K_2 & 0 & 0 & 0 & 0 & -M^{-1}K_{pd} & 0 & 0 & 0 & 0 & -M^{-1}K_{p\delta e} \\ -T'_{do}{}^{-1}K_4 & 0 & -T'_{do}{}^{-1}K_3 & T'_{do}{}^{-1} & 0 & 0 & 0 & -T'_{do}{}^{-1}K_{qd} & 0 & 0 & 0 & 0 & -T'_{do}{}^{-1}K_{q\delta e} \\ -T_A^{-1}K_A K_5 & 0 & -T_A^{-1}K_A K_6 & -T_A^{-1} & T_A^{-1}K_A & 0 & 0 & -T_A^{-1}K_A K_{vd} & 0 & 0 & 0 & 0 & -T_A^{-1}K_A K_{v\delta e} \\ M^{-1}\gamma^2 K_{PSS} K_1 & M^{-1}\gamma^2 K_{PSS} D & M^{-1}\gamma^2 K_{PSS} K_2 & 0 & -\eta\sqrt{\gamma} & \eta\sqrt{\gamma}(1-\gamma) & T_w^{-1}\gamma(\eta\sqrt{\gamma}T_w - \gamma) & -M^{-1}\gamma^2 K_{PSS} K_{pd} & 0 & 0 & 0 & 0 & -M^{-1}\gamma^2 K_{PSS} K_{p\delta e} \\ M^{-1}\gamma K_{PSS} K_1 & M^{-1}\gamma K_{PSS} D & M^{-1}\gamma K_{PSS} K_2 & 0 & 0 & -\eta\sqrt{\gamma} & T_w^{-1}(\eta\sqrt{\gamma}T_w - \gamma) & -M^{-1}\gamma K_{PSS} K_{pd} & 0 & 0 & 0 & 0 & -M^{-1}\gamma K_{PSS} K_{p\delta e} \\ M^{-1}K_{PSS} K_1 & M^{-1}K_{PSS} D & M^{-1}K_{PSS} K_2 & 0 & 0 & 0 & -T_w^{-1} & -M^{-1}K_{PSS} K_{pd} & 0 & 0 & 0 & 0 & -M^{-1}K_{PSS} K_{p\delta e} \\ K_7 & 0 & K_8 & 0 & 0 & 0 & 0 & -K_9 & 0 & 0 & 0 & 0 & K_{c\delta e} \\ -K\alpha^2 K_{1,ij}/M_i & -K\alpha^2 D_i/M_i & -K\alpha^2 K_{2,ij}/M_i & 0 & 0 & 0 & 0 & -K\alpha^2 K_{pd,i}/M_i & -\beta\sqrt{\alpha} & \beta\sqrt{\alpha}(1-\alpha) & \alpha(\beta\sqrt{\alpha}T_{wi} - \alpha)/T_{wi} & 0 & -K\alpha^2 K_{p\delta e}/M_i \\ -K\alpha K_{1,ij}/M_i & -K\alpha D_i/M_i & -K\alpha K_{2,ij}/M_i & 0 & 0 & 0 & 0 & -K\alpha K_{pd,i}/M_i & 0 & -\beta\sqrt{\alpha} & (\beta\sqrt{\alpha}T_w - \alpha)/T_{wi} & 0 & -K\alpha K_{p\delta e}/M_i \\ -KK_{1,ij}/M_i & -KD_i/M_i & -KK_{2,ij}/M_i & 0 & 0 & 0 & 0 & -KK_{pd,i}/M_i & 0 & 0 & -1/T_{wi} & 0 & -KK_{p\delta e}/M_i \\ 0 & 0 & 0 & 0 & 0 & 0 & 0 & -K_s K_{dP}/T_s & K_s/T_s & 0 & 0 & 0 & -1/T_s \end{bmatrix} \quad (8)$$

parameters (i.e. genes) that will be optimized (i.e. $\gamma, \eta, K_{PSS}, K, \alpha, \beta, K_{dP}, \ell_o$). Here, ℓ_o is a vector with each element of ℓ_o representing PSSs' number and their locations in the closed-loop system. It also indicates the UPFC location on a fixed line. The upper and lower bounds on the variables are also specified. For this problem, the parameters of the stabilizers and their locations are used to maximize a set of N objective, each representing N PSSs (N is a number of machines equipped with PSSs), [24]. i.e.

$$f(x) = [f_1(x), f_2(x), \dots, f_N(x)] \quad (9)$$

The set of objectives $f(x)$ is subjected to a bound of constraints

$$L_i \leq x_i \leq U_i \quad (10)$$

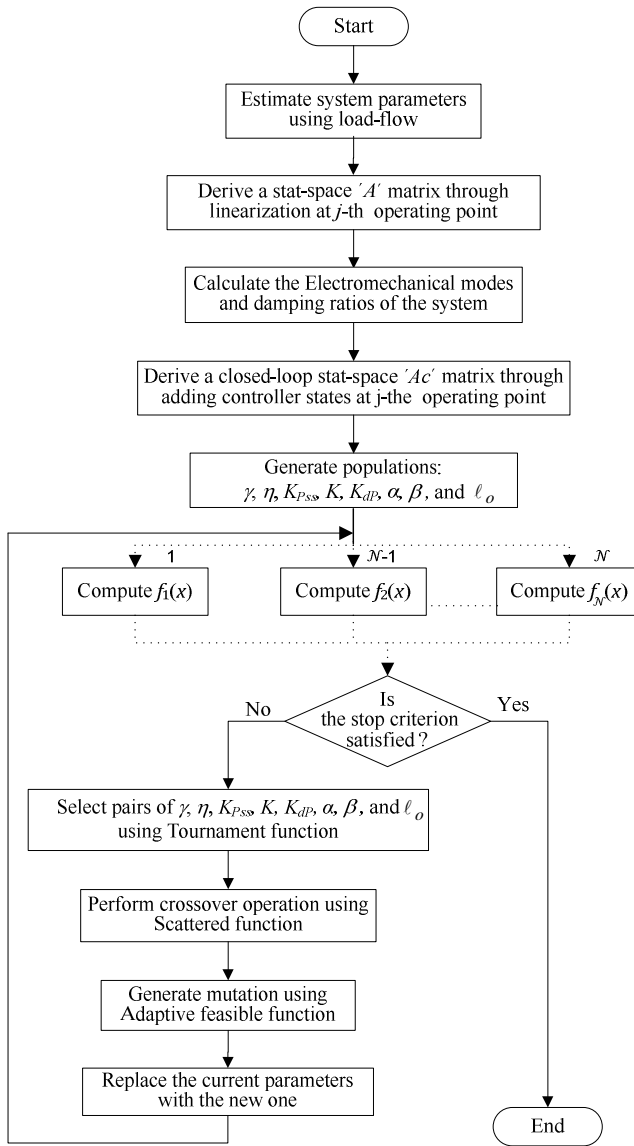


Fig. 3. Flowchart of the proposed algorithm using GA.

where x_i is a decision variable, and, U_i and L_i are the upper, and lower bounds on the parameters of the stabilizers and their locations respectively.

In order to characterize the objectives, the Pareto optimality has to be utilized, since no unique solution to the problem exists. Here, each $f(x)$ component is competing to maximize the minimum damping ratio of a closed-loop system with some number of PSSs. Therefore, for $f_k(x)$, a single component of $f(x)$, we have

$$\max_{f_k(x)} = \min \left(\left[\zeta_{i,j} \right]_k \right) \quad (11)$$

where $\zeta_{i,j}$ is the damping ratio of the i -th eigenvalue of the j -th operating condition and $k = 1, 2, \dots, N$.

Then, out of the optimization results (values of the objective function and values of the system parameters), the algorithm selects the best result for each component of $f(x)$. These selected parameters are then used to create a new generation using the processes discussed in [25] for selection, crossover, and mutation operations. This is mainly done to ensure that the search is not trapped at a local minima.

To achieve this, pairs of chromosomes are elected based on their scaled values from $f(x)$ for mating. For better formation results, the proposed algorithm uses a random selection tournament function to choose a small subset of chromosomes and appoint the better fitness chromosome in that particular subset as a parent. The tournament function is chosen because it provides excellent performance when the population is large, as in our application, and it does not need to sort it. After a number trials, the best size of the tournament, which specifies the number of chromosomes, is found to be 4. Subsequently, the new child (offspring chromosome) of the new generation is created using the crossover operation that combines the two parents (chromosomes). Typically, a crossover probability values from 0.6 to 1.0 provides best results [26]. In this work, trials revealed that a crossover probability of 0.9 is found to be quite satisfactory. A scattering function is used to create a random binary vector and eventually select the genes for PSSs, UPFC-based stabilizer parameters, and ℓ_o . It does that from the first and second parents. For example, if the binary vector is $[0 \ 0 \ 1 \ 1 \ 0 \ 1 \ 1 \ 0 \ 1]$, then the first parent is $[\gamma_{2m}, \eta_{2m}, K_{PSS,2m}, K_{PSS,3m}, K_m, \alpha_m, \beta_m, K_{dP,m}, \ell_{o,1m}, \ell_{o,2m}]$, and the second parent is $[\gamma_{2n}, \eta_{2n}, K_{PSS,2n}, K_{PSS,3n}, K_n, \alpha_n, \beta_n, K_{dP,n}, \ell_{o,1n}, \ell_{o,2n}]$, and therefore the function returns the child $[\gamma_{2n}, \eta_{2n}, K_{PSS,2m}, K_{PSS,3m}, K_n, \alpha_m, \beta_m, K_{dP,m}, \ell_{o,1n}, \ell_{o,2m}]$.

To produce the new generation, the mutation process flips randomly selected genes from individual parents to create the children. The adaptive feasible function is selected for the mutation process to randomly take the directions that adaptively follow the last generation. In addition, to satisfy the linear constraints and bounds, a step length is chosen along each direction.

IV. RESULTS AND DISCUSSIONS

The proposed method has been tested on the 16-machine 68-bus New-England and New-York interconnected system. The single line diagram of the system is shown in Fig. 4. Each generator can be installed with a PSS. The data of the system are given in [23]. In order to guarantee the robustness of the proposed approach, several scenarios have been used in the optimization process and tested with the scenarios that were not used in the training process. A load-flow program is conducted for five different scenarios to estimate the initial system conditions, including the base case and the four line outage-scenarios. These conditions, which were also considered in [11], can be described as

- Scenario 1: Base case.
- Scenario 2: outage of line 28-29.
- Scenario 3: outage of line 1-2
- Scenario 4: outage of line 25-26 and line 3-18.
- Scenario 5: outage of line 41-42.

The electromechanical modes and the damping ratio of the system without stabilizers for the base case, and other conditions, are depicted in Fig. 5. The results showed that a system without a controller is unstable for all scenarios.

A. Application of GA

The process of applying GA is divided into two steps as discussed below:

Step 1: the proposed GA based optimization technique is applied to determine the optimal location of the UPFC. All lines are selected to fit with the UPFC considering only the nominal operating condition. In addition, all possible locations of the controller's input signals are considered.

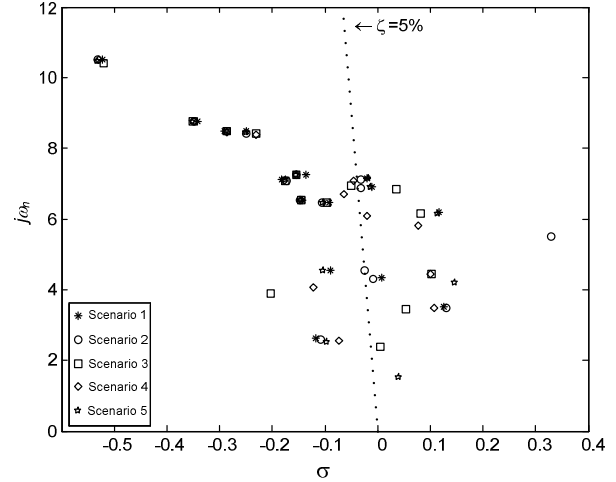


Fig. 5. Eigenvalues associated with electromechanical modes without controller for five scenario-conditions.

The number of population is selected to be 100 based on several trial runs with different set of populations. In the simulation, the output started converging and remained stable after about 100 generations. Therefore, the stopping criterion is selected to be 200 as an extra measure. The results show that the optimal location of the UPFC is at line 46-49, followed by line 50-51. The lead-lag controller's input signal is taken from G16 when the UPFC is located on line 46-49. Fig. 4 shows the location of the UPFC on line 46-49.

Step 2: The GA-based optimization method is used to simultaneously tune PSSs parameters (i.e. K_{PSS} , γ , and η), as well as determining their optimal locations (using ℓ_o) and minimum numbers, and tuning the UPFC damping controller

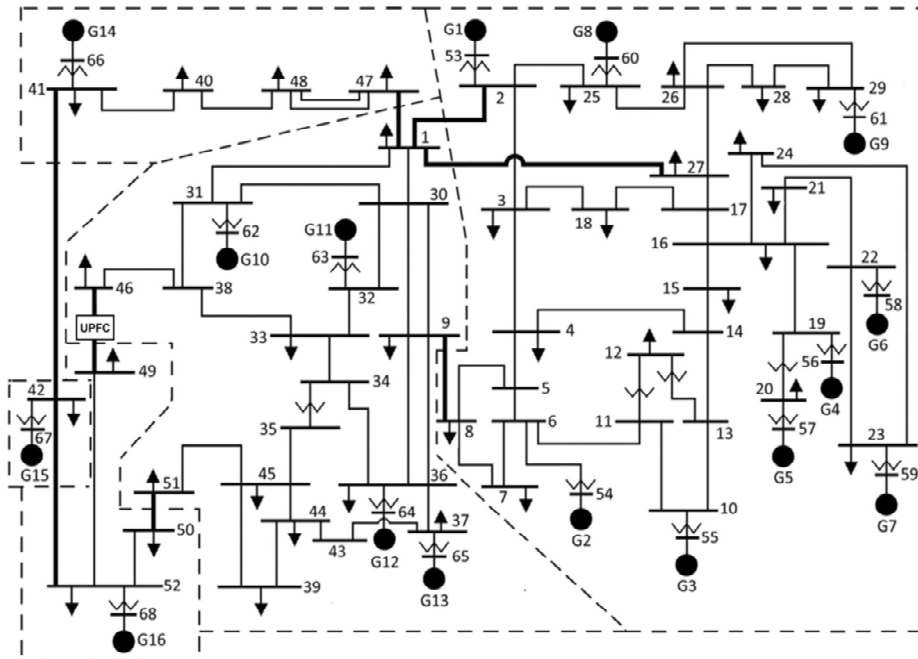


Fig. 4. A single line diagram of the 16-machine 68-bus New-England and New-York interconnected system.

parameters (i.e. α , β , K , and K_{dp}), whilst considering different operating conditions. All possible combinations of the PSSs' locations have been considered. Combinations of PSSs' locations are shown in Fig. 6.

Each chromosome has 68 individual genes, as shown in Fig. 7. Based on several trial runs with different set of populations, 100 individuals are selected as the population size for each generation. In other words, the GA creates an initial population of chromosome by filling 100 rows with 68 parameters that should be optimized. The stop criterion is selected to be 300, representing the maximum since the output started converging and remained stable after about 200 generations. The typical values of the upper and lower bounds on each parameter of the damping controller are given in Table I. Theoretically, the controller gain bounds can take values that ranges $-\infty$ to $+\infty$. However, in this paper the bounds are set to narrower bounds; $[-50 \ 50]$ for controller parameter K and $[-20 \ 20]$ for controller parameter K_{dp} in order to improve the GA performance. In addition, and for the same reason, the bounds for parameters (α , β , γ_i , and η_i) are set within acceptable limits around values found in the literature of UPFCs and PSSs, [11, 12, 20].

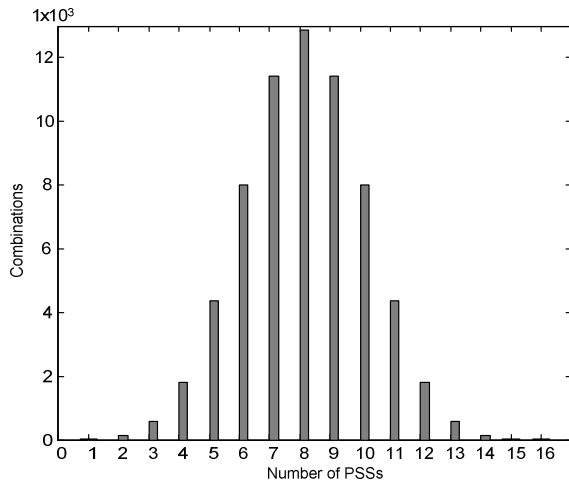


Fig. 6. Combinations of PSSs' locations.

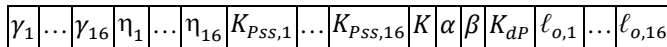


Fig. 7. A chromosome for the problem of tuning PSSs parameters, with their optimal location and minimum numbers, and tuning the UPFC damping controller parameters.

	K	α	β	K_{dp}	$K_{PSS,i}$	γ_i	η_i
Lower	-50	0.1	1	-20	0.1	0.1	1.2
Upper	50	12	16	20	50	13	16

The minimum damping ratio for the overall operating conditions of the electromechanical modes when the UPFC is located on line 46-49 and line 50-51 separately are shown in Fig. 8. The results show that the UPFC provides better performance when it is located on line 46-49 compared to when it is on line 50-51. These results agree with those obtained in Step 1.

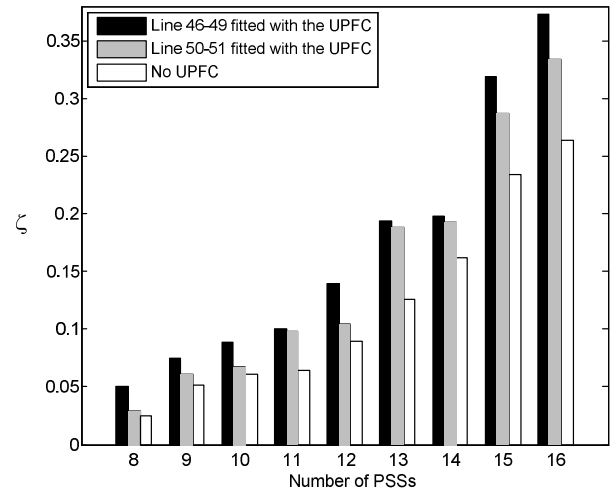


Fig. 8. Damping ratio comparison for the system with and without the UPFC.

The electromechanical modes of a closed-loop system with the UPFC installed on line 46-49 are calculated and depicted in Fig. 9. The results show that damping ratios increase with increasing number of PSSs.

The parameters and locations of the PSSs are shown in Figs. 10-12, while the optimal parameters of the UPFC damping controller are shown in Table II. Starting with 8, up to 16 generators are shown in Figs. 10-12 and Table II. In Figs. 10-12, under the 'Number of PSSs' axis, each number indicates the number of PSSs selected for optimization. For example, under the PSSs of 8, generators 1, 3, 7, 9, 10, 12, 15, and 16 are selected by the GA to be equipped with PSSs.

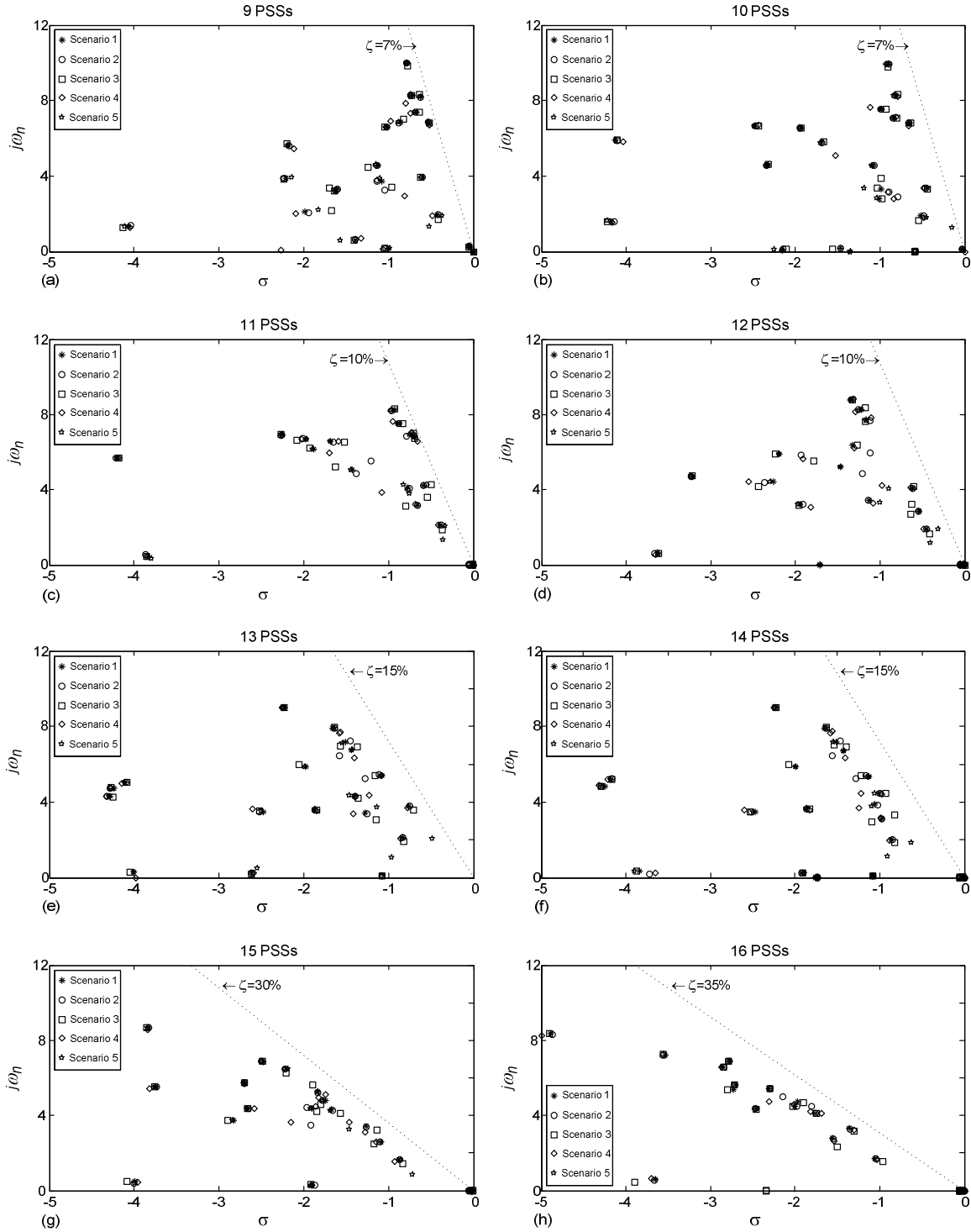


Fig. 9. Electromechanical modes of the system equipped with the UPFC and different numbers of PSSs for five scenario-conditions.

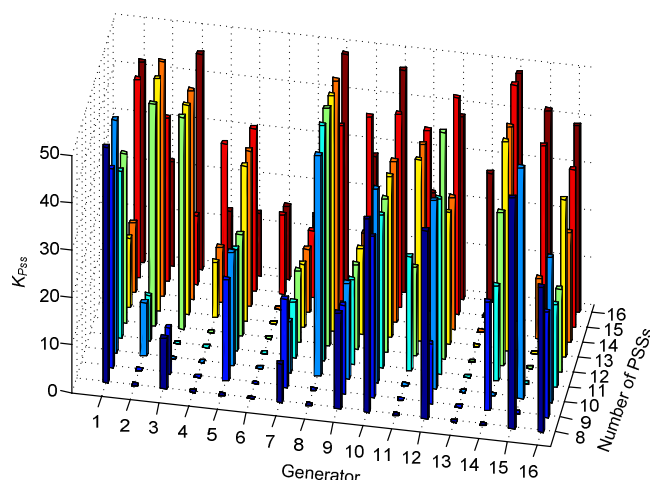


Fig. 10. Gain K_{PSS} of PSSs when the system with the UPFC installed.

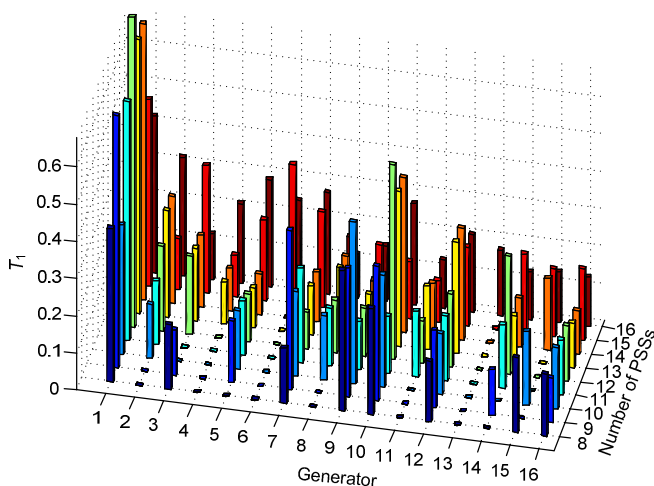


Fig. 11. Time constant T_1 of PSSs when the system with the UPFC installed.

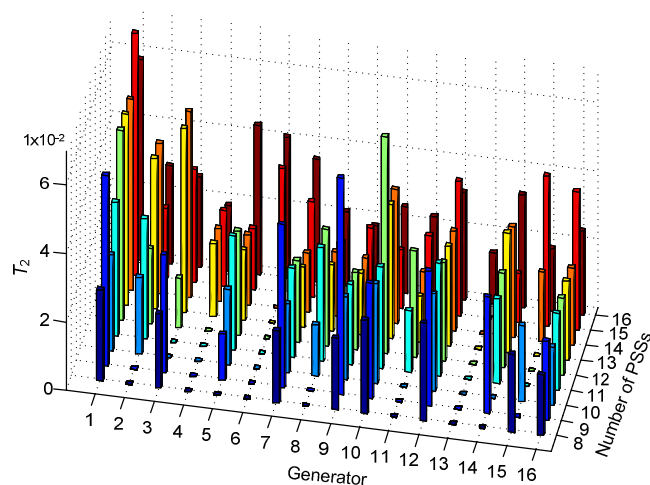


Fig. 12. Time constant T_2 of PSSs when the system with the UPFC installed.

TABLE II
OPTIMAL PARAMETERS OF THE UPFC DAMPING CONTROLLER

Number of PSSs	T_a	T_b	K	K_{dP}
8	2.6527	0.3635	7.6951	-0.2069
9	1.1567	0.2441	8.2125	-0.0099
10	2.4993	0.3425	7.9861	-0.8319
11	0.2071	0.1224	3.1529	-4.6658
12	0.2224	0.1104	4.3798	-2.6524
13	0.3436	0.9390	1.4320	-7.6608
14	0.3390	0.9266	1.4476	-2.8518
15	0.0874	0.0972	1.0347	-14.2882
16	0.3390	0.9266	1.2550	-4.4437

B. Transient Stability Analysis

To test the effectiveness of the approach, four different contingencies are applied on different lines at different areas, shown in Table III. In all contingencies, a six-cycle three-phase fault is applied at 0 sec, and the fault is cleared after 100 ms.

TABLE III
CONTINGENCIES USED TO SHOW THE SYSTEM TRANSIENT RESPONSES

Contingency no.	Description
First	Three-phase fault on line 28-29 at bus 28
Second	Three-phase fault on line 41-42 at bus 41
Third	Three-phase fault on line 1-27, load increase by 25% at bus 27, and generation increased by 20% at G8
Fourth	Three-phase fault line 8-9 (bus 9), load increased by 25% at bus 9, and generation increased by 5% at G12

The generator speed deviation during the faults, when the UPFC and 9 PSSs are installed in the system, are shown in Fig. 13. The results demonstrate that the system is sufficiently dampen under all fault contingencies.

It is well known that the voltage control of the DC link capacitor inside the UPFC interacts negatively with the PSS. The proposed design using GA for coordination among the PSSs, and between PSSs and UPFC, stabilizes this negative interaction. This is achieved by determining the optimal location of the UPFC while tuning its control parameters, resulting in the optimization of the quantity, parameters and locations of PSSs under different operating conditions. The coordinated design regains a satisfactory damping of power system oscillations as demonstrated in the results presented in this paper. Figures 14 and 15 show the UPFC DC voltage deviation, the excitation angle change $\Delta\delta_E$ and the speed deviation of G1 during the first fault contingency using the proposed method and basic control method (without coordination). It is clear from these figures that the DC voltage is well controlled through modulating the excitation angle δ_E and the system is sufficiently stable when the proposed optimization approach is used. While the system with the proposed coordination takes about 6 seconds to damp out the oscillation, the uncoordinated system takes longer time (around 18 seconds) to damp the oscillations due to the negative interaction of the DC link capacitor with PSS.

C. Advantages of adding UPFC to the system

The system with PSSs and UPFC installed is compared to a system with only PSSs installed in terms of:

(a) Damping Ratio

In the coordinated design between PSSs and the UPFC, the minimum damping ratio is increased, compared to the system installed with only PSSs, as shown in Fig. 8.

(b) PSSs Number

Adding the UPFC with an optimal damping controller to

the system can reduce the number of PSSs. Fig. 8 shows that to achieve 0.05 damping, the system that is installed with UPFC needs to be equipped with 8 PSSs, while the system without the UPFC installed needs to be equipped with 9 PSSs. However, in order to achieve a damping of 0.075, the system with UPFC installed needs to be equipped with 9 PSSs and the system without UPFC needs to be equipped with 12 PSSs.

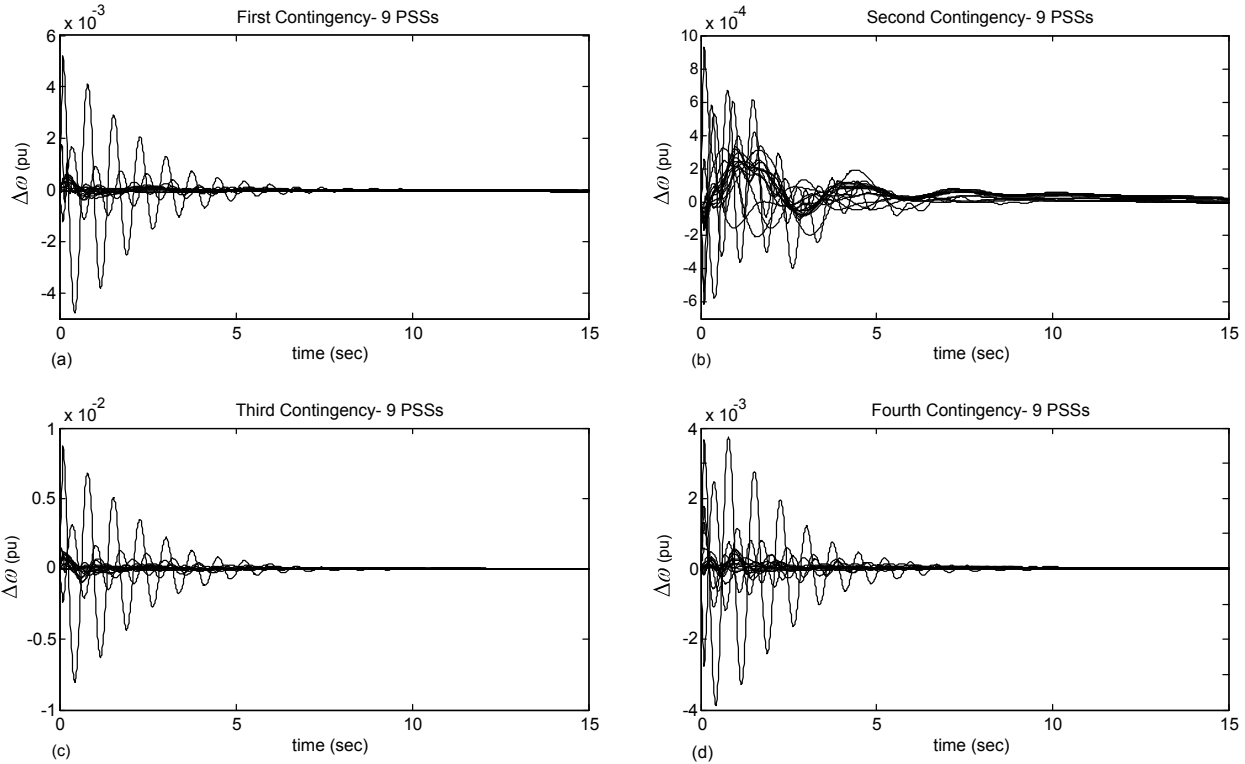


Fig. 13. Generator speed deviation responses when the system installed with the UPFC-based stabilizer and 9 PSSs is subjected to different fault contingencies.

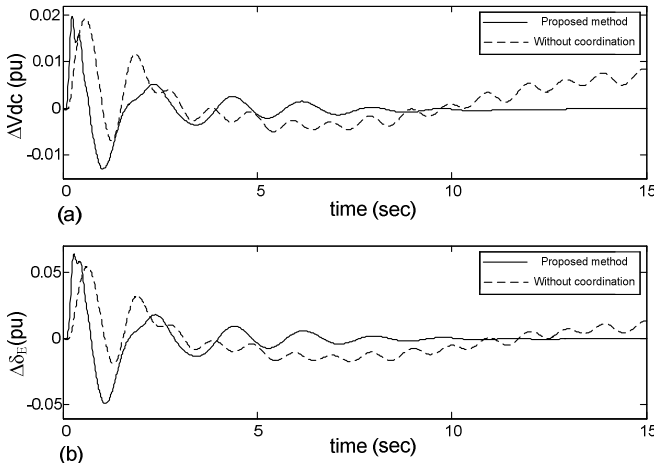


Fig. 14. DC voltage deviation and the excitation phase angle deviation with and without coordination when the system is subjected to the first fault contingency.

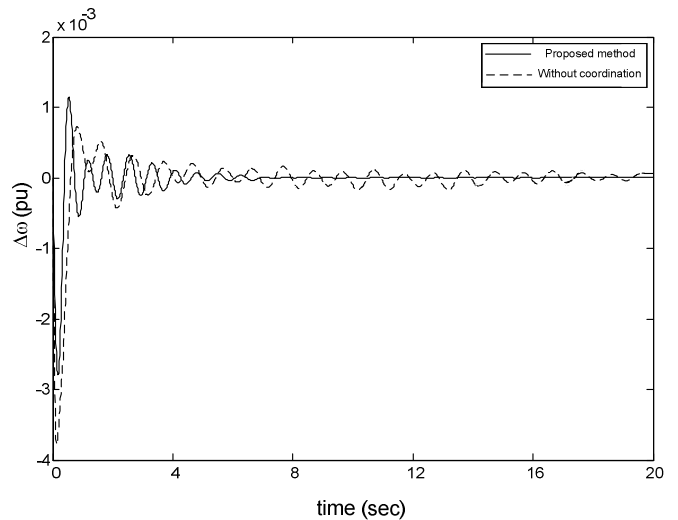


Fig. 15. G1's Speed deviation with and without coordination when the system is subjected to the first fault contingency.

V. CONCLUSION

Using a criterion based on the damping ratio, an optimization algorithm was successfully applied to establish the optimal coordination between PSSs and UPFC-based stabilizer using Genetic Algorithm (GA). A multi-objective function was utilized to formulate the problem, whose solution aims to maximize the damping ratios of the electromechanical modes using different combinations of PSSs with UPFC. The proposed optimization technique was applied to tune the parameters of the UPFC damping controller and the PSSs, determine the optimal location of the UPFC, find out the optimal locations of PSSs, and minimize the number of required PSSs under different operating conditions. The approach was tested on the 16-machine in 68-bus New England-New York interconnected system, and its effectiveness was established during the Eigenvalue analysis and nonlinear simulation results. In addition, the results demonstrated that the minimum damping ratio can be increased, and the number of PSSs can be reduced by adding UPFC-based stabilizer to the system.

REFERENCES

- [1] L. H. Hassan, M. Moghavvemi, H. A. F. Almurib, and O. Steinmayer, "Current state of neural networks applications in power system monitoring and control," *Int. J. Electr. Power Energy Syst.*, vol. 51, pp. 134-144, 2013.
- [2] M. J. Basler and R. C. Schaefer, "Understanding power-system stability," *IEEE Trans. Ind. Appl.*, vol. 44, pp. 463-474, 2008.
- [3] M. Kashki, Y. L. Abdel-Magid, and M. A. Abido, "Parameter optimization of multimachine power system conventional stabilizers using CDCARLA method," *Int. J. Electr. Power Energy Syst.*, vol. 32, pp. 498-506, 2010.
- [4] L. H. Hassan, M. Moghavvemi, H. A. F. Almurib, K. M. Muttaqi, and H. Du, "Damping of low-frequency oscillations and improving power system stability via auto-tuned PI stabilizer using Takagi-Sugeno fuzzy logic," *Int. J. Electr. Power Energy Syst.*, vol. 38, pp. 72-83, 2012.
- [5] A. El-Zonkoly, "Optimal sizing of SSSC controllers to minimize transmission loss and a novel model of SSSC to study transient response," *Electr. Power Syst. Res.*, vol. 78, pp. 1856-1864, 2008.
- [6] S. Gerbex, R. Cherkaoui, and A. Germond, "Optimal location of multi-type FACTS devices in a power system by means of genetic algorithms," *IEEE Power Eng. Rev.*, vol. 21, pp. 59-60, 2001.
- [7] L. H. Hassan, M. Moghavvemi, and H. A. F. Mohamed, "Takagi-Sugeno fuzzy gains scheduled PI controller for enhancement of power system stability," *Am. J. Appl. Sci.*, vol. 7, pp. 145-152, 2010.
- [8] Y. Song and A. Johns, *Flexible AC Transmission Systems (FACTS)*. Cornwall: International Ltd. Padstow, 1999.
- [9] L. Khan and K. L. Lo, "Hybrid micro-GA based FLCs for TCSC and UPFC in a multi-machine environment," *Electr. Power Syst. Res.*, vol. 76, pp. 832-843, 2006.
- [10] B. K. Kumar, S. N. Singh, and S. C. Srivastava, "Placement of FACTS controllers using modal controllability indices to damp out power system oscillations," *IET Gener. Transm. Distrib.*, vol. 1, pp. 209-217, 2007.
- [11] K. Sebaa and M. Boudour, "Optimal locations and tuning of robust power system stabilizer using genetic algorithms," *Electr. Power Syst. Res.*, vol. 79, pp. 406-416, 2009.
- [12] H. F. Wang, "Applications of modelling UPFC into multi-machine power systems," *IEE Proc. Gener. Transm. Distrib.*, vol. 146, pp. 306-312, 1999.
- [13] Y. L. Abdel-Magid and M. A. Abido, "Robust coordinated design of excitation and TCSC-based stabilizers using genetic algorithms," *Electr. Power Syst. Res.*, vol. 69, pp. 129-141, 2004.
- [14] H. I. Shaheen, G. I. Rashed, and S. J. Cheng, "Application and comparison of computational intelligence techniques for optimal location and parameter setting of UPFC," *Eng. Appl. Artif. Intell.*, vol. 23, pp. 203-216, 2010.
- [15] M. E. El-Hawary, *Electric Power Applications of Fuzzy Systems*. New York: IEEE Press, 1998.
- [16] S. Mishra, "Neural-network-based adaptive UPFC for improving transient stability performance of power system," *IEEE Trans. Neural Networks*, vol. 17, pp. 461-470, 2006.
- [17] M. A. Abido, "Pole placement technique for PSS and TCSC-based stabilizer design using simulated annealing," *Int. J. Electr. Power Energy Syst.*, vol. 22, pp. 543-554, 2000.
- [18] M. A. Abido and Y. L. Abdel-Magid, "Coordinated design of a PSS and an SVC-based controller to enhance power system stability," *Int. J. Electr. Power Energy Syst.*, vol. 25, pp. 695-704, 2003.
- [19] L. Hassan, M. Moghavvemi, and H. F. Almurib, "Modeling UPFC into Multi-Machine Power Systems," *Arabian J. Sci. Eng.*, vol. 37, pp. 1613-1624, 2012.
- [20] A. T. Al-Awami, Y. L. Abdel-Magid, and M. A. Abido, "A particle-swarm-based approach of power system stability enhancement with unified power flow controller," *Int. J. Electr. Power Energy Syst.*, vol. 29, pp. 251-259, 2007.
- [21] L. H. Hassan, M. Moghavvemi, and H. A. F. Mohamed, "Impact of UPFC-based damping controller on dynamic stability of Iraqi power network," *Sci. Res. Essays*, vol. 6, pp. 136-145, 2011.
- [22] P. M. Anderson and A. A. Fouad, Eds., *Power System Control and Stability*, Second. ed.: Wiley-IEEE Press, 2003.
- [23] G. Rogers, *Power System Oscillations*: Springer, 1999.
- [24] K. Deb, *Multi-Objective Optimization using Evolutionary Algorithms*. Chichester: John Wiley & Sons, Ltd, 2001.
- [25] M. Negnevitsky, *Artificial Intelligence A Guide to Intelligent Systems*, Second. ed.: Addison-Wesley, 2002.
- [26] I. Robandi, K. Nishimori, R. Nishimura, and N. Ishihara, "Optimal feedback control design using genetic algorithm in multimachine power system," *Int. J. Electr. Power Energy Syst.*, vol. 23, pp. 263-271, 2001.



Lokman H. Hassan (S'08-M'13) obtained his BSc and MSc in Power Engineering from the University of Technology, Baghdad and PhD from University of Malaya, Malaysia. He joined University of Duhok, Kurdistan Region, Iraq in 2002 and currently he is a lecturer in the Department of Electrical and Computer Engineering. He worked as a project engineer for seven years before he became a lecturer. His main research interests are control systems design, monitoring, stability and power system control.



Mahmoud Moghavvemi received the Bsc. and MSc. from State University of New York at Buffalo and University of Bridgeport in 1986 and 1988. He worked as test and design engineer for CTI Electronics USA and director of Informatics school of engineering prior to joining Department of Electrical Engineering of University of Malaya as a lecturer in 1991. He pursued his PhD in the same department and graduated with

distinction in 1995. He was promoted to the post of associated Professor in 1996 and to full professor in 2002. His contributions can be seen in more than 30 patents, more than 200 refereed journals and conference articles and many post graduate students. Professor Moghavvemi is the reviewer for several distinguished journals in his field of expertise. He is the founder and currently the director of the center for Research in Applied Electronics (CRAE).



Haider A. F. Almurib (S'00–M'05–SM'11) received his PhD in electrical engineering from the University of Malaya, Kuala Lumpur, Malaysia, in 2006. He is currently working as a Professor in the Department of Electrical and Electronic Engineering, The University of Nottingham, Kuala

Lumpur where he lead the Electrical Systems and Applied Mathematics (ESAM) research division for a while before taking the head of department position. Before this he was a Lecturer in the University of Malaya. He also worked in industry for four years as an R&D engineer in the field of computer automation. His research interests include nonlinear intelligent control, electric machines & drives, embedded systems, fault tolerance of digital systems, and nanoelectronics.

Kashem M. Muttaqi (M'01, SM'05) received the B.Sc. degree in electrical and electronic engineering from Bangladesh University of Engineering and Technology (BUET), Bangladesh in 1993, the M.Eng.Sc. degree in electrical engineering from University of Malaya, Malaysia in 1996 and the Ph.D. degree



in Electrical Engineering from Multimedia University, Malaysia in 2001. Currently, he is an Associate Professor at the School of Electrical, Computer, and Telecommunications Engineering, and member of Australian Power Quality and Reliability (APQRC) at the University of Wollongong, Australia. He was associated with the University of Tasmania, Australia as a Research Fellow/Lecturer/Senior Lecturer from 2002 to 2007, and with the Queensland University of Technology, Australia as a Research Fellow from 2000 to 2002. Previously, he also worked for Multimedia University as a Lecturer for three years. He has more than 17 years of academic experience and has authored or coauthored over 165 papers in international journals and conference proceedings. His research interests include distributed generation, renewable energy, electrical vehicles, smart-grid, power system planning and control. Dr. Muttaqi is an Associate Editor of the IEEE Transactions on Industry Applications.